

# Enhanced photocathode performance through optimization of film thickness and substrate

Anna Alexander Nathan A. Moody Prabhakar R. Bandaru

Citation: *Journal of Vacuum Science & Technology B, Nanotechnology and Microelectronics: Materials, Processing, Measurement, and Phenomena* **35**, 022202 (2017); doi: 10.1116/1.4976527

View online: <http://dx.doi.org/10.1116/1.4976527>

View Table of Contents: <http://avs.scitation.org/toc/jvb/35/2>

Published by the [American Vacuum Society](#)

---

## Articles you may be interested in

[Bright and durable field-emission source derived from frozen refractory-metal Taylor cones](#)

*Journal of Vacuum Science & Technology B, Nanotechnology and Microelectronics: Materials, Processing, Measurement, and Phenomena* **35**, 02C10602C106 (2017); 10.1116/1.4976536

[Electrical properties of Cs<sub>3</sub>Sb photocathode emitters in panel device applications](#)

*Journal of Vacuum Science & Technology B, Nanotechnology and Microelectronics: Materials, Processing, Measurement, and Phenomena* **35**, 02C10802C108 (2017); 10.1116/1.4977582

[Gas-phase diagnostics during H<sub>2</sub> and H<sub>2</sub>O plasma treatment of SnO<sub>2</sub> nanomaterials: Implications for surface modification](#)

*Journal of Vacuum Science & Technology B, Nanotechnology and Microelectronics: Materials, Processing, Measurement, and Phenomena* **35**, 021802021802 (2017); 10.1116/1.4976534

[In situ study of graphene crystallinity effect on field electron emission characteristics](#)

*Journal of Vacuum Science & Technology B, Nanotechnology and Microelectronics: Materials, Processing, Measurement, and Phenomena* **35**, 02C10702C107 (2017); 10.1116/1.4977546

---

**HIDEN**  
ANALYTICAL

## Instruments for Advanced Science

Contact Hiden Analytical for further details:

**W** [www.HidenAnalytical.com](http://www.HidenAnalytical.com)  
**E** [info@hiden.co.uk](mailto:info@hiden.co.uk)

[CLICK TO VIEW](#) our product catalogue



### Gas Analysis

- › dynamic measurement of reaction gas streams
- › catalysis and thermal analysis
- › molecular beam studies
- › dissolved species probes
- › fermentation, environmental and ecological studies



### Surface Science

- › UHV TPD
- › SIMS
- › end point detection in ion beam etch
- › elemental imaging - surface mapping



### Plasma Diagnostics

- › plasma source characterization
- › etch and deposition process reaction
- › kinetic studies
- › analysis of neutral and radical species



### Vacuum Analysis

- › partial pressure measurement and control of process gases
- › reactive sputter process control
- › vacuum diagnostics
- › vacuum coating process monitoring

# Enhanced photocathode performance through optimization of film thickness and substrate

Anna Alexander

Program in Materials Science, Department of Mechanical Engineering, University of California, San Diego, La Jolla, California 92093

Nathan A. Moody

Los Alamos National Laboratory, Los Alamos, New Mexico 87545

Prabhakar R. Bandaru<sup>a)</sup>

Program in Materials Science, Department of Mechanical Engineering, University of California, San Diego, La Jolla, California 92093

(Received 27 November 2016; accepted 30 January 2017; published 22 February 2017)

It is shown that the efficiency of photoelectron emission may be enhanced, several-fold, through optimization of photocathode film thickness and appropriate substrate configuration. Such an enhancement is based on a careful consideration of wave interference effects in the film and the consequent modulation of the absorption profiles and electron emission probabilities. The inadequacy of the well-known Lambert-Beer law for modeling photon absorption in thin films is also discussed. © 2017 American Vacuum Society. [<http://dx.doi.org/10.1116/1.4976527>]

## I. INTRODUCTION

Electron emission from photocathodes (PC) involves the ejection of electrons subsequent to photon absorption<sup>1</sup> and is used for a variety of applications<sup>2</sup> ranging from photomultiplier tubes,<sup>3,4</sup> free electron lasers,<sup>5</sup> photoemissive detectors,<sup>1</sup> and linear accelerator systems.<sup>6</sup> Generally, the emission has been modeled following a three-step process<sup>7</sup> involving successive steps related to the (1) *absorption* of an incident photon by the electron, followed by the (2) transport of the excited electrons *to* the surface, and finally (3) the *emission* of the electron *from* the surface. The efficacy of such a process is dictated by the average number of electrons emitted for a given photon, and has been considered through the quantum efficiency (QE).<sup>8</sup> While metal photocathodes are chemically stable and exhibit faster response times, they suffer from a poor QE ( $\ll 1\%$ ).<sup>9</sup> Alternately, low work function semiconductor based photocathode materials<sup>4</sup> are used for their relatively larger QE ( $\sim 12\%$ ).<sup>9</sup>

A major goal of photocathode research is an enhancement of the QE, and/or a reduction in intrinsic beam emittance (related to the product of the beam size and its angular spread). An important design criterion for the photocathode involves the consideration that the electron excitation by incident photons, needs to occur within the electron escape depth ( $\lambda_{esc}$ ), which then dictates a target photocathode thickness. Consequently, most photocathode films (typically deposited on stainless steel or tungsten substrates  $>100 \mu\text{m}$  thick) in usage are of the order of 10–50 nm thick,<sup>10–13</sup> with larger thickness being used for higher absorption due to presumed reduced influence of grain boundaries, or are optimized *in situ* during film growth,<sup>14</sup> without much quantitative rationale.<sup>10</sup> Additionally, insufficient attention<sup>15</sup> has been paid to the specific geometric influences of the film and thickness as a function of a specific substrate, with respect to

possible interference effects,<sup>16,17</sup> which may modulate significantly both the incident light absorption and the electron emission efficiency. Enhanced light absorption arises through carefully matching the impedance of the photocathode–substrate system to that of the vacuum to which electrons are emitted. We have observed, for instance, that absorption could be increased by an order of magnitude through proper design. Moreover, we find that the often-used Lambert-Beer (L-B) law may not be a reliable indicator of the extent of absorption in many configurations. We discuss such effects with the focus on improving the QE of photocathodes. The paper focuses on reflection mode photocathodes, and not on transmission mode devices, as the former is most commonly used. Additionally, emittance considerations, while important, are outside the scope of the paper.

Given that flat photocathode surfaces are typically preferred: Fig. 1, as rough surfaces increase emittance,<sup>9</sup> it is posited that minimizing reflections at the various interfaces (i.e., vacuum–photocathode film, film–substrate) would be beneficial for enhanced photon absorption. In this context, one may consider typical antireflecting film characteristics commonly used in optical applications through the deployment of selective destructive interference.<sup>18</sup> However, the photon absorption processes, (1) for the conversion of photons to excite electrons in the photocathode film, and (2) in the substrate/metal, due to the imaginary component of the refractive index, imply the need for different design principles.

Through a careful review of previous work,<sup>19–21</sup> we hypothesized that the reflection of energy from the substrate and redeposition into the photocathode—along with reducing transmission through the substrate, could be beneficial. In this paper, we predict quantitatively the specific criteria through which such benefits could be harnessed through modeling characteristics of a typical low electron affinity  $\text{K}_2\text{CsSb}$  photocathode film,<sup>22</sup> at an incident wavelength of 532 nm.

<sup>a)</sup>Electronic mail: pbandaru@ucsd.edu

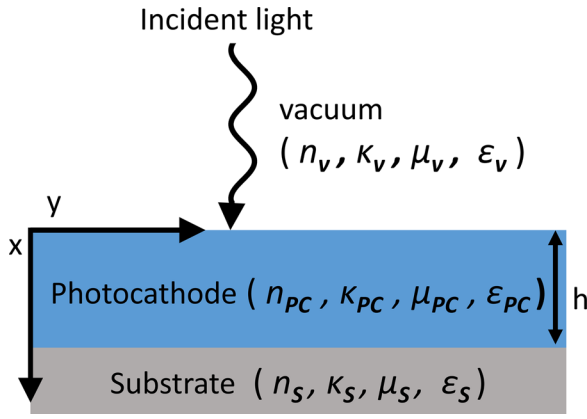


FIG. 1. (Color online) Schematic of a typical photoemission system configuration indicating light incidence (of a specific wavelength:  $\lambda$ , say 532 nm) onto a photocathode film deposited on a substrate. The complex refractive index ( $\tilde{n} = n + i\kappa$ ) as well as the dielectric permittivity ( $\epsilon$ ) and magnetic permeability ( $\mu$ ) of the vacuum (V), PC film, and substrate (S) are indicated.

## II. METHODS

In describing the photon absorption processes in a photocathode film of thickness:  $h$ , for facilitating subsequent photoemission into the vacuum (V), the net absorption coefficient:  $A$  would be related to the detailed absorption profile— $a(x)$  through the thickness of the film ( $x$ )—see Fig. 1 for axes orientation—by

$$A = \int_0^h a(x) dx. \quad (1)$$

The materials (PC, and substrate: S) are each described through a respective complex refractive index:  $\tilde{n} = n + i\kappa$ . Considering normal incidence of photons (e.g., through laser illumination from vacuum): Fig. 1, the reflection coefficients at vacuum–photocathode film interface (i.e.,  $r_{V-PC}$ ) and the photocathode film–substrate interface (i.e.,  $r_{PC-S}$ ) are the Fresnel coefficients,<sup>23</sup> i.e.,

$$r_{V-PC} = \frac{\tilde{n}_V - \tilde{n}_{PC}}{\tilde{n}_V + \tilde{n}_{PC}}, \quad (2a)$$

$$r_{PC-S} = \frac{\tilde{n}_{PC} - \tilde{n}_S}{\tilde{n}_{PC} + \tilde{n}_S}. \quad (2b)$$

The electric field in the photocathode film is

$$E_y = E_o e^{i\omega t} (1 + r_{V-PC}) e^{i\tilde{n}_{PC} k x}. \quad (3)$$

The magnetic field ( $H_z$ ) could then be derived from  $H = (-1/\mu) \int \nabla \times E dt$ , to be

$$H_z = - \left( \frac{E_o}{\omega \mu_o \mu_{PC}} \right) \tilde{n}_{PC} k e^{i\omega t} (1 + r_{V-PC}) e^{i\tilde{n}_{PC} k x}. \quad (4)$$

While the net power density flow into the material could be parameterized through the Poynting vector in the complex form,<sup>24</sup> ( $S_x$ ) =  $1/2 E_y \cdot H_z^*$ , where  $H_z^*$  is the complex conjugate of  $H_z$ , we define a differential power density ( $P_a$ ) to describe the power absorption through the thickness of the material, as:  $P_a = \nabla \cdot \text{Re}(S_x)$ , as

$$P_a = - \left( \frac{\kappa_{PC} k^2 \tilde{n}_{PC}^*}{\omega \mu_o \mu_{PC}} \right) |E_o (1 + r_{V-PC})|^2 e^{-(x/\lambda_{opt})}. \quad (5)$$

The  $\lambda_{opt} = 1/(2k\kappa_{PC})$  and is related to a characteristic decay length of the  $P_a$ . The input power ( $P_{in}$ ), at  $x = 0$ , is

$$P_{in} = - \left( \frac{k \tilde{n}_{vac}}{2\omega \mu_o \mu_V} \right) |E_o|^2. \quad (6)$$

The absorption profile,  $a(x) = P_a/P_{in}$ , would be

$$a(x) = - \left( \frac{2\kappa_{PC} k \tilde{n}_{PC}^*}{\mu_{PC}} \right) |(1 + r_{V-PC})|^2 e^{-(x/\lambda_{opt})}. \quad (7)$$

Equation (7) may be alternately written in accord with the well-known L-B relation

$$a(x) = I_o e^{-(x/\lambda_{opt})}, \quad (8)$$

with  $I_o = (2\kappa_{PC} k \tilde{n}_{PC}^* / \mu_{PC}) |(1 + r_{V-PC})|^2$ .

However, such derivations do not particularly consider back-reflections and interactions of the waves in the PC film. For a finite film thickness of  $h$ , considering the forward and backward waves yields an alternate relation for the electric field, as

$$E_x = E_o e^{i\omega t} (c_f e^{i\tilde{n}_{PC} k x} + c_b e^{-i\tilde{n}_{PC} k x}). \quad (9)$$

Here,  $c_f (= (1 + r_{V-PC}) / (1 - r_{V-PC} r_{PC-S} e^{2i\tilde{n}_{PC} k h}))$  and  $c_b (= c_f r_{PC-S} e^{2i\tilde{n}_{PC} k h})$  denote the amplitude of the contributions from the forward and backward traveling waves, respectively. Consequently, considering the differential power density through the Poynting relationship, etc., we derive a modified absorption profile of the form

$$a(x) = I_o^f |e^{-(x/2\lambda_{opt})} + r_{PC-S} e^{2i\tilde{n}_{PC} k h} e^{(x/2\lambda_{opt})}|^2, \quad (10)$$

where  $I_o^f = ((1 + r_{V-PC}) / (1 - r_{V-PC} r_{PC-S} e^{2i\tilde{n}_{PC} k h}))^2 (2k\kappa_{PC} \tilde{n}_{PC}^* / \omega \mu_{PC})$ .

It can be observed that Eq. (10) reduces to the form of Eq. (8) when  $\tilde{n}_{PC}$  is purely imaginary and  $\tilde{n}_{PC} k h \gg 1$ . In this case,  $c_b$  approaches zero with the implication that the backward traveling wave does not influence the electric field in the PC film. Essentially, this is equivalent to assuming an infinitely thick film and it is evident that the L-B relation implicitly incorporates such an assumption. As we have previously discussed that PC films have thickness of the order of 10–50 nm—due to constraints related to the electromagnetic skin depth as well as the electron escape depth (see Table I for optical constants related to typically used films), we posit that the L-B relation is not accurate and instead forms such as Eq. (10) to be deployed for assessing the absorption profiles of PC films. Consequently, many extant theoretical models of photoemission<sup>10–12,25</sup> may need to be modified. The second term in Eq. (10) is most indicative of finite film thickness effects, and at a  $(h/\lambda_{opt})$  ratio close to unity, there would be substantial reflected wave amplitude which may influence the  $a(x)$  and photoemission.

TABLE I. Optical constants of various commonly used photocathode films: (i) Cs<sub>3</sub>Sb (Ref. 31), (ii) K<sub>2</sub>CsSb (Refs. 22 and 32), (iii) CsTe (Ref. 33), and (iv) the multialkali S20 photocathode (Refs. 32 and 34). The computed electromagnetic skin depth values at the respective wavelengths ( $\lambda$ ) are indicated in parentheses.

Cathode material	Refractive index (skin depth)			
	$\lambda$ : 532 nm	$\lambda$ : 405 nm	$\lambda$ : 355 nm	$\lambda$ : 266 nm
Cs <sub>3</sub> Sb	0.3 + 0.9i (44 nm)	0.6 + 0.4i (87 nm)		
K <sub>2</sub> CsSb	3.2 + 0.8i (52 nm)	2.2 + 1.2i (27 nm)	1.6 + 1.3i (21 nm)	1.3 + 0.6i (34 nm)
CsTe				0.8 + 0.8i (28 nm)
S20	2.9 + 0.4i (106 nm)	2.8 + 0.6i (57 nm)	2.2 + 0.2i (128 nm)	2.1 + 0.1i (163 nm)

### III. RESULTS AND DISCUSSION

We plot the absorption coefficient,  $A$ , computed from incorporating Eq. (10) in Eq. (1) for various substrates (with varying  $r_{PC-S}$ ) in Fig. 2(a). Several aspects related to such graphs are to be noted, e.g., an  $A$  maximum (1) occurs at a specific thickness, i.e., at  $h_{max}$ , into the film and *not* at the surface, as would be expected from the L-B relation, (2) is sensitive to the particular substrate, i.e., Ag: Fig. 2(b), W: Fig. 2(c), and Al: Fig. 2(d), on which the PC film is deposited. Specifically, the  $h_{max}$  is  $\sim 28$  nm (for Al substrate),  $\sim 20$  nm (for Ag and Cu substrates),  $\sim 18$  nm (for Au substrate), and  $\sim 42$  nm (for W substrate). Also noted in Fig. 2(a) is the  $A$  calculated assuming an infinitely thick film, i.e., with  $h = \infty$ , as the upper limit to the integral in Eq. (1). Moreover, PC films of similar  $A$  have differing  $a(x)$  profiles and consequently, the thickness corresponding to the maximum in  $a(x)$  is different from  $h_{max}$ . For example, deploying a K<sub>2</sub>CsSb film on a Ag substrate results in a  $h_{max}$  of  $\sim 20$  nm, while  $a(x)$  is largest for  $h \sim 14$  nm. Generally, for  $h < h_{max}$ , the maximum in  $a(x)$  is at the surface while for  $h > h_{max}$ , the maximum is *in* the film. A plausible reason is that the  $A$  is

enhanced when the forward and the reflected waves are  $\pi$  radians out of phase at the vacuum side of the V-PC interface. Changing the substrate (see Table II for the optical constants of the various metal substrates typically used in photoemission studies) influences the specific thickness at which maxima in  $A$  and  $a(x)$  occur due to the variation of  $r_{PC-S}$ . Generally, a high substrate reflectivity would enhance interference effects in the PC film and contribute to enhanced absorption.

It is pertinent to consider, from Figs. 2(b)–2(d), that  $a(x)$  variation is much more involved compared to what would be expected from the L-B relation which specifies an exponential drop in the absorption from the surface through the film thickness. The latter aspect could be rationalized through the neglect of backwards traveling waves. While the  $a(x)$  magnitude seems to be larger than that estimated from the L-B relation for certain specific values of  $h$  (typically less than  $h_{max}$ ), the overall  $A$  is nevertheless smaller due to the smaller upper limit of the integral in Eq. (1). Alternately, for  $h > h_{max}$ , the L-B solution generally overestimates  $a(x)$ .

We will now extend such insights into  $a(x)$  variation to the respective influences on the QE of photoemission. In a basic model, while the incident photons penetrate the PC film–substrate system to an average distance corresponding to the electromagnetic skin-depth ( $\sim \lambda_{opt}$ ), only the electrons excited at a depth equivalent to  $\lambda_{esc}$  are eligible to drift to the PC–vacuum interface. A larger  $\lambda_{esc}$  implies a greater likelihood of the electrons escaping from the photocathode<sup>26,27</sup> and an increased  $F_e$ . As electron–electron scattering is predominant for metals,  $\lambda_{opt}$  may be taken as equivalent to  $\lambda_{esc}$ . However, for semiconductors, the scattering time is more difficult to determine due to alternate scattering mechanisms,<sup>28</sup> e.g., to electron–lattice scattering in addition to

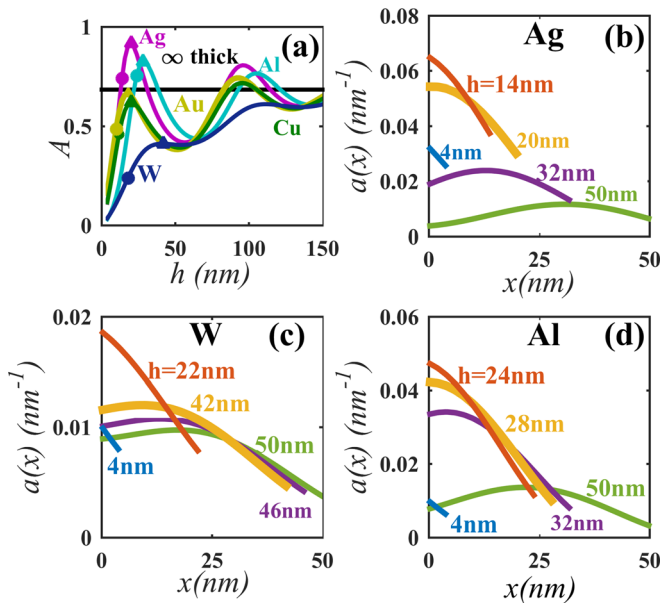


FIG. 2. (Color online) (a) Plot of the absorption coefficient:  $A$ , as a function of photocathode film thickness ( $h$ ) for various substrates, i.e., Ag: (b), W: (c), and Al: (d), on which the photocathode film is deposited. Also noted in (a) is the  $A$  calculated assuming an infinitely thick film, i.e., assuming  $h = \infty$ .

TABLE II. Refractive index of metals that are typically used as substrates for photocathode films (Ref. 35).

Substrate metal	Refractive index			
	532 nm	405 nm	355 nm	266 nm
Al	0.9 + 6.0i	0.5 + 4.8i	0.3 + 4.2i	0.2 + 3.1i
Ag	0.2 + 3.1i	0.1 + 1.9i	0.2 + 1.3i	0.8 + 1.5i
Au	0.5 + 2.1i	1.5 + 1.8i	1.6 + 1.8i	1.6 + 1.9i
Cu	0.8 + 2.5i	1.3 + 2.3i	1.2 + 1.9i	1.5 + 1.7i
W	3.5 + 2.7i	3.2 + 2.5i	3.2 + 2.5i	2.8 + 2.6i

electron–electron scattering, etc., which precludes an explicit relation between  $\lambda_{opt}$  and  $\lambda_{esc}$ .

However, as previously discussed, Eq. (10) is more valid and was applied for assessing the probability ( $F_e$ ) of a photoexcited electron reaching the surface, through

$$F_e = \int_0^h a(x)e^{-(x/\lambda_{esc})} dx. \quad (11)$$

It is then indicated clearly through Eq. (11) that, for a given  $a(x)$ , electrons excited closer to the surface (smaller  $x$ ) would have a greater probability of photoemission. The evaluation of  $F_e$  hinges on the knowing  $\lambda_{esc}$ , which is not a well-characterized quantity. While more accurately known for metals (e.g., the  $\lambda_{esc}$  has been reported<sup>8,29,30</sup> as  $\sim 4$  nm for Al and  $\sim 5.5$  nm for Cu at an incident wavelength of 250 nm), for semiconductor photocathodes, the  $\lambda_{esc}$  is larger<sup>10,19</sup> and in the range of 20–40 nm. We plot  $F_e$  for such a range considering specific  $a(x)$  variation for Ag: Fig. 3(a), Al: Fig. 3(b), and W: Fig. 3(c) substrates. A general feature is the convergence of the  $F_e$  at larger values of  $h$  due to the dominating influence of  $\lambda_{esc}$ . A much higher  $F_e$  is evident for photocathode films deposited on Ag substrates in comparison to those deposited on W substrates for  $h \leq 25$  nm. However, the  $F_e$  in the latter seems to be less sensitive to film thickness variation. Generally, W has larger transmission (and less back-reflected waves) compared to Ag or Al implying a concomitant smaller influence on the  $F_e$ . We also indicate, for comparison, in Fig. 3(d) the corresponding variation of the  $F_e$  assuming the complete absence of the back-reflected waves, which yields a constant value only dependent on the  $\lambda_{esc}$ . From comparing Figs. 3(d) and 3(a), it is observed that the  $F_e$  can be enhanced threefold (i.e., from  $\sim 0.24$  to  $\sim 0.76$

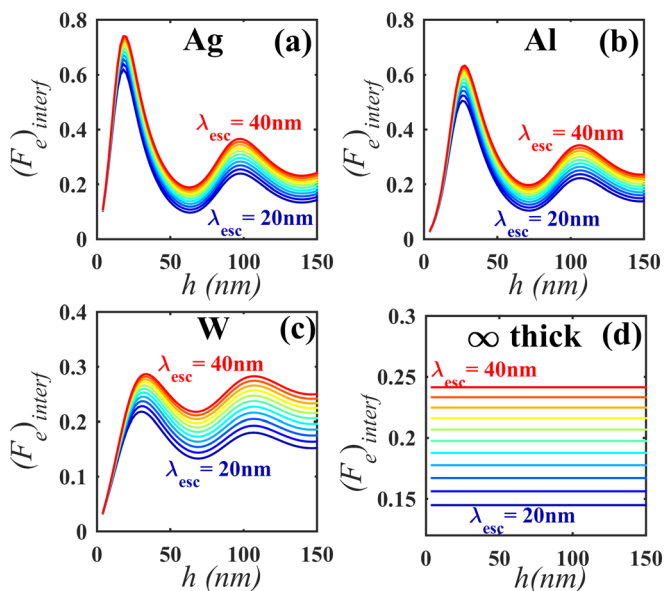


FIG. 3. (Color online) Probability ( $F_e$ ) of a photoexcited electron reaching the surface, as a function of photocathode film thickness ( $h$ ) and electron escape depth ( $\lambda_{esc}$ ) for various substrates, i.e., (a) Ag, (b) W, (c) Al, and (d) the corresponding variation of the  $F_e$  assuming the complete absence of the back-reflected waves, which yields a constant value only dependent on  $\lambda_{esc}$ .

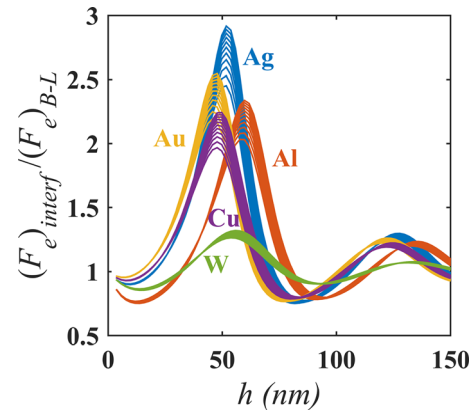


FIG. 4. (Color online) Plot of the  $(F_e)_{interf}/(F_e)_{L-B}$  ratio, relating the electron emission probability considering interference effects to the emission probability in the absence of such effects. A ratio more (less) than unity implies that the use of the traditional Lambert-Beer relation under-(over-)estimates the likelihood of photoemission. The individual curves are for varying values of  $\lambda_{esc}$  in the range of 20 nm (top) to 40 nm (bottom).

for  $\lambda_{esc} = 40$  nm with Ag substrates) through such considerations.

We now discuss the implications on the QE of photoemission, considering interference effects and the proper variation of  $a(x)$ , relative to the case where such interferences are not considered (as in the L-B relation), i.e.,  $(F_e)_{interf}/(F_e)_{L-B}$  in Fig. 4. The contrast arises from taking into account the finite thickness of the film and consequent interference effects, which modify the electric field intensities as, specified through Eq. (10). A ratio more (less) than unity implies that the use of the traditional L-B relation under-(over-)estimates the likelihood of photoemission. This is evident from the figure for a range of film thicknesses and is also shown to be sensitive to the substrate. Additionally, since photocathodes are rarely atomically flat, it is also useful to consider the influence of roughness. Generally, for  $\lambda_{opt} \ll \lambda_{esc}$ , the only requirement is that the wave must be sufficiently decayed such that any interference effects do not change the  $A$ , implying a film thickness,  $h$  of the order of  $3 \lambda_{opt}$ . When  $\lambda_{opt} > \lambda_{esc}$ , the shape of the  $a(x)$  curve matters, but only for depths shallow enough that the electrons can actually be emitted. The relevant thickness can be derived through using Eq. (10) and yields  $h \sim 3 \lambda_{opt}$ .

Generally, the discussed principles underlying interference enhanced photoemission should be valid for other materials combinations as well to various degree,<sup>16,17</sup> specifically depending on the complex refractive index variation (which in turn is wavelength sensitive) between the film and the substrate. A general rule of thumb may be that, at a given wavelength, the  $r_{PC-S}$  should be large to minimize the energy transmitted into the substrate. Additionally, the  $n_{PC}$  and the  $\kappa_{PC}$  influences the  $a(x)$  by changing the periodicity in  $A$  and the amplitude decay rates, respectively, and would need to be considered.

## IV. CONCLUSIONS

In summary, we have proposed that electron emission from photocathode thin films could be significantly

enhanced—by as much as a factor of three through a comprehensive consideration of the influence of film substrates and interference effects in the films. The influence of the finite thickness of the films as well as the complex refractive indices of the film and the substrate plays a major role in obtaining such enhancement. Experiments on photocathode films, with well-controlled thicknesses, indicating (1) enhanced QE with Al or Ag substrates, as well as (2) QE variability with film thickness, would validate the models indicated in our paper.

## ACKNOWLEDGMENTS

The authors are grateful for financial support from the LANL-UCSD initiative. The authors appreciate discussions with H. Yamada on the EM modeling.

- <sup>1</sup>G. H. Rieke, *Detection of Light: From the Ultraviolet to the Submillimeter* (Cambridge University, Cambridge, 1994).
- <sup>2</sup>G. R. Fleming and M. A. Ratner, *Phys. Today* **61**(7), 28 (2008).
- <sup>3</sup>H. Photonics, *Photomultiplier Tubes: Basics & Applications* (Hamamatsu Photonics, 2007).
- <sup>4</sup>J. I. Pankove, *Optical Processes in Semiconductors* (Dover, New York, 1971).
- <sup>5</sup>C. Brau, *Free-Electron Lasers* (Academic, Boston, MA, 1990).
- <sup>6</sup>D. H. Dowell and J. F. Schmerge, *Phys. Rev. Spec. Top.—Accel. Beams* **12**, 074201 (2009).
- <sup>7</sup>C. Berglund and W. Spicer, *Phys. Rev.* **136**, A1030 (1964).
- <sup>8</sup>A. Alexander, N. A. Moody, and P. R. Bandaru, *J. Vac. Sci. Technol., A* **34**, 021401 (2016).
- <sup>9</sup>D. H. Dowell *et al.*, *Nucl. Instruments Methods Phys. Res., Sect. A* **622**, 685 (2010).
- <sup>10</sup>P. D. Townsend, R. Downey, S. W. Harmer, Y. Wang, A. Cormack, R. Mcalpine, and T. Bauer, *J. Phys. D: Appl. Phys.* **39**, 1525 (2006).
- <sup>11</sup>K. L. Jensen, P. G. O'Shea, and D. W. Feldman, *Appl. Phys. Lett.* **81**, 3867 (2002).
- <sup>12</sup>K. L. Jensen, N. A. Moody, D. W. Feldman, E. J. Montgomery, and P. G. O'Shea, *J. Appl. Phys.* **102**, 074902 (2007).
- <sup>13</sup>L. Cultrera, C. Gulliford, A. Bartnik, H. Lee, and I. Bazarov, *Appl. Phys. Lett.* **108**, 134105 (2016).
- <sup>14</sup>L. Cultrera, S. Karkare, B. Lillard, A. Bartnik, I. Bazarov, B. Dunham, W. Schaff, and K. Smolenski, *Appl. Phys. Lett.* **103**, 103504 (2013).
- <sup>15</sup>H.-S. Jeong, *Trans. Electr. Electron. Mater.* **17**, 306 (2016).
- <sup>16</sup>K. Sahasrabudde, J. W. Schwede, I. Bargatin, J. Jean, R. T. Howe, Z.-X. Shen, and N. A. Melosh, *J. Appl. Phys.* **112**, 094907 (2012).
- <sup>17</sup>W. Liu, Y. Chen, W. Lu, A. Moy, M. Poelker, M. Stutzman, and S. Zhang, *Appl. Phys. Lett.* **109**, 252104 (2016).
- <sup>18</sup>G. R. Fowles, *Introduction to Modern Optics*, 2nd ed. (Dover, New York, 1975).
- <sup>19</sup>J. A. Love and J. R. Sizelove, *Appl. Opt.* **7**, 11 (1968).
- <sup>20</sup>E. G. Ramberg, *Appl. Opt.* **6**, 2163 (1967).
- <sup>21</sup>M. A. Novice and J. Vine, *Appl. Opt.* **6**, 1171 (1967).
- <sup>22</sup>D. Motta and S. Schönert, *Nucl. Instruments Methods Phys. Res., Sect. A* **539**, 217 (2005).
- <sup>23</sup>W. Chang, *Principles of Optics for Engineers* (Cambridge University, Cambridge, MA, 2015).
- <sup>24</sup>J. D. Jackson, *Classical Electrodynamics* (Wiley, New York, 1999).
- <sup>25</sup>W. E. Spicer and A. Herrera-Gomez, *Proc. SPIE* **2022**, 18 (1993).
- <sup>26</sup>J. A. Knapp, F. J. Himpsel, and D. E. Eastman, *Phys. Rev. B* **19**, 4952 (1979).
- <sup>27</sup>W. F. Krolikowski and W. E. Spicer, *Phys. Rev.* **185**, 882 (1969).
- <sup>28</sup>K. L. Jensen, B. L. Jensen, E. J. Montgomery, D. W. Feldman, P. G. O'Shea, and N. Moody, *J. Appl. Phys.* **104**, 044907 (2008).
- <sup>29</sup>D. R. Lide, *CRC Handbook Chemistry and Physics*, 85th ed. (BocaRaton, FL, 2004).
- <sup>30</sup>D. H. Dowell, F. K. King, R. E. Kirby, and J. F. Schmerge, *Phys. Rev. Spec. Top.—Accel. Beams* **9**, 063502 (2006).
- <sup>31</sup>S. M. Johnson, *Appl. Opt.* **32**, 2262 (1993).
- <sup>32</sup>S. W. Harmer, R. Downey, Y. Wang, and P. D. Townsend, *Nucl. Instruments Methods Phys. Res., Sect. A* **564**, 439 (2006).
- <sup>33</sup>S. M. Johnson, *Appl. Opt.* **31**, 2332 (1992).
- <sup>34</sup>S. Hallensleben, S. Harmer, and P. Townsend, *Opt. Commun.* **180**, 89 (2000).
- <sup>35</sup>A. D. Rakić, A. B. Djurišić, J. M. Elazar, and M. L. Majewski, *Appl. Opt.* **37**, 5271 (1998).